Radical mechanism of cyanophage phycoerythrobilin synthase (PebS)

Andrea W. U. Busch, Edward J Reijerse, Wolfgang Lubitz, Eckhard Hofmann, Nicole Frankenberg-Dinkel

RADICAL MECHANISM OF CYANOPHAGE PHYCOERYTHROBILIN SYNTHASE (PebS)

Andrea W. U. Busch[1] , Edward J. Reijerse[2], Wolfgang Lubitz[2], Eckhard Hofmann[3] and Nicole Frankenberg-Dinkel[1]

[1]Physiology of Microorganisms, Faculty of Biology and Biotechnology, Ruhr-University Bochum, 44780 Bochum, Germany
[2]Max-Planck-Institute for Bioinorganic Chemistry, 45470 Mülheim an der Ruhr, Germany
[3] Biophysics, Faculty of Biology and Biotechnology, Ruhr-University Bochum, 44780 Bochum, Germany,

Running title: Radical mechanism of PebS

Key words: bilin reductase, open-chain tetrapyrrole, EPR, radical, phycoerythrobilin synthase

Address correspondence to:
Nicole Frankenberg-Dinkel
Ruhr-University Bochum
Physiology of Microorganisms
44780 Bochum
Germany
Fax: ++49 - (0)234 - 32-14620
E-mail: nicole.frankenberg@rub.de

Abbreviations: BV, biliverdin IXα; DVBV, dihydrobiliverdin, Fd, ferredoxin; FDBR, ferredoxin-dependent bilin reductase; FNR, ferredoxin-$NADP^+$-oxidoreductase; PBS, phycobilisome; PCB, phycocyanobilin; PEB, phycoerythrobilin; PebS, phycoerythrobilin synthase; PΦB, phytochromobilin; WT, wild type.

SYNOPSIS

Phycoerythrobilin (PEB) is a pink-colored open-chain tetrapyrrole molecule found in the cyanobacterial light-harvesting phycobilisome. Within the phycobilisome, PEB is covalently bound via thioether bonds to conserved cysteine residues of the phycobiliprotein subunits. In cyanobacteria, biosynthesis of PEB proceeds via two subsequent two-electron reductions catalyzed by the ferredoxin-dependent bilin reductases (FDBR) PebA and PebB starting from the open-chain tetrapyrrole biliverdin IXα. Recently, a new member of the FDBR family was identified in the genome of a marine cyanophage. In contrast to the cyanobacterial enzymes, PEB-synthase (PebS) from cyanophage combines both two-electron reductions for PEB synthesis. Here we show that PebS acts via a substrate radical mechanism and that two conserved aspartate residues at position 105 and 206 are critical for stereospecific substrate protonation and conversion. Based on the crystal structures of both PebS variants and presented biochemical and biophysical data a mechanism for BV conversion to PEB is postulated and discussed with respect to other FDBR family members.

INTRODUCTION

Cyanobacteria form a large and diverse group of photoautotrophic bacteria that contribute significantly to the global primary production. They efficiently harvest light via their antenna complexes, the phycobilisomes (PBS[1]) [1]. One major chromophore incorporated into the PBS is phycoerythrobilin (PEB), a pink-colored open-chain tetrapyrrole molecule (phycobilin). The biosynthesis of PEB starts with the oxidative cleavage of heme by heme oxygenase to yield biliverdin IXα (BV) [2]. Further reduction of BV is then catalyzed by ferredoxin-dependent bilin reductases (FDBRs) [3]. As the name implies electrons are provided by the one-electron transferring redox protein ferredoxin (Fd). FDBRs are a class of radical enzymes that do not possess any metal or organic cofactors [3-5]. They catalyze not only the biosynthesis of PEB, but also of the phycobilins phycocyanobilin (PCB) and phytochromobilin (PΦB), the chromophore of plant phytochromes [3, 6] (Fig. 1).

FDBRs can be subdivided into two classes depending on the number of electrons transferred to the substrate. One class is catalyzing two-electron reductions, the other one four-electron reductions. In plants, PΦB synthesis proceeds via a two-electron reduction at the A-ring position catalyzed by PΦB synthase (HY2) [7]. In cyanobacteria PEB synthesis requires two sequential two-electron reductions: 15,16-dihydrobiliverdin:ferredoxin oxidoreductase (PebA) reduces the substrate BV at the 15,16-methine bridge of the D-ring to the intermediate 15,16-dihydrobiliverdin (15,16-DHBV) which is further reduced in a second two-electron reduction step to the final product PEB by PEB:ferredoxin oxidoreductase (PebB) [8]. In contrast, PCB synthesis is catalyzed by PCB:ferredoxin oxidoreductase (PcyA) in a formal four-electron reduction combining 18^1, 18^2-DHBV:ferredoxin oxidoreductase activity and PCB:ferredoxin oxidoreductase activity. Here, the D-ring exovinyl reduction yielding the intermediate 18^1,18^2-DHBV precedes the A-ring reduction yielding the final product PCB [4] (Fig.1). These reduction steps were shown to proceed via bilin radical intermediates and similar results were obtained for the *Arabidopsis thaliana* FDBR HY2 [5, 9, 10]. A second FDBR able to catalyze a four-electron reduction was discovered in the genome of the *Prochlorococcus* infecting cyanophage P-SSM2 [11]. First annotated as a PebA, the enzyme is able to catalyze the synthesis of PEB with BV as the substrate in a formal four-electron reduction with 15,16-DHBV as the intermediate. Due to its novel properties it was named PEB-synthase (PebS) [12]. PebS combines the activities of cyanobacterial PebA and PebB in one enzyme which has not been found in a cyanobacterium yet [12]. PebS is a single globular protein with an α-β-α sandwich fold and high structural similarity to PcyA, the best studied member of the FDBR family. The structure revealed amino acid residues likely to be involved in substrate conversion and possible proton transfer [13]. These residues comprise two aspartate residues at position 105 and 206 that are also highly conserved in the whole FDBR family [9]. The D105 residue has been suggested to be involved in initial protonation of the BV substrate to facilitate subsequent electron transfer from Fd [13]. Here we present evidence that PebS catalyzed PEB synthesis indeed proceeds via a radical mechanism and that both aspartate residues are important for stereospecific substrate protonation and conversion.

EXPERIMENTAL

Materials — All chemicals were American Chemical Society grade or better unless specified otherwise. All assay components were purchased from Sigma, Munich. Glutathione-Sepharose™ 4FF, PreScission Protease and expression vector pGEX-6P-3 were obtained from GE Healthcare,

Munich. Alternatively, Protino® Glutathione Agarose 4B from Macherey-Nagel (Düren) was used. HPLC-grade acetone, acetonitrile, formic acid, and spectroanalytical grade glycerol were obtained from J. T. Baker Inc., Griesheim. Sep-Pak Light cartridges were obtained from Waters, Eschborn. BV IXα was obtained from Frontier Scientific, Carnforth, Lancashire, UK.

Protein expression, purification, and site-directed mutagenesis — PebS from cyanophage P-SSM2, Fd from *Synechococcus sp.* PCC 7002 (Fd_{7002}) or cyanophage P-SSM2 ($Fd_{P\text{-}SSM2}$) were recombinantly expressed and purified as described previously [12]. Purified Fd was dialyzed against 25 mM TES-KOH (pH 8.0), 100 mM KCl and 15 % glycerol and stored at -20 °C. The concentration was determined as described in [12].
All site-directed mutants of PebS were generated in pGEX_*pebS*_P-SSM2 [12] using the QuikChange® site-directed mutagenesis kit (Stratagene, Waldbronn) using the following primers (shown is only the forward primer, the reverse primer is the complement, introduced base pair changes are underlined): D105N: 5′-CTTGTTTTGGTATGAACCTGATGAAGTTTAGTG-3′; D105E: CTTGTTTTGGTATGGAACTGATGAAGTTTAGTG; D206N: 5′-CTTATATGACTGAACTTAATCCTGTTAGAG-3′; D206E: CTTATATGACTGAACTTGAACCTGTTAGAGG. PebS variants were expressed and purified following the method used for the wild-type protein.

Preparation of bilins — Preparative production of chromophores was performed under anaerobic conditions as described earlier with the following modifications [5]. Ferredoxin-NADP(H)-reductase from *Synechococcus sp.* PCC7002 (FNR) and $Fd_{P\text{-}SSM2}$ or Fd_{7002} were used in varying concentrations. PebS concentrations ranged from 10 - 200 µM. The assay was carried out at 20 °C and substrate was added sequentially in excess amounts. The reaction was started with an NADPH-regenerating system with final concentrations of 2.2 mM glucose-6-phosphate, 27 µM $NADP^+$ and 0.37 U/ml glucose-6-phosphate-dehydrogenase. The reaction was stopped and the products purified according to [8]. 15,16-DHBV was prepared with PebA from *Synechococcus sp.* WH8020 [8] or respective PebS variants unable to perform 15,16-DHBV reduction. 15,16-DHBV was then purified according to the protocol used before [8]. Product formation was verified via HPLC.

Spectroscopic analysis of bilin reductase activity — Anaerobic bilin reductase assays were performed utilizing an Agilent 8453 UV-Visible Spectrophotometer as described previously [5] with the following modifications. Assay conditions consisted of 25 mM TES-KOH (pH 8.0), 100 mM KCl, 0.01 µM FNR from *Synechococcus sp.* PCC7002 and 1 µM $Fd_{P\text{-}SSM2}$, 10 µM bovine serum albumin, 10 µM BV, 10 µM purified wild-type or PebS variant, 50 U/ml glucose oxidase, 100 mM glucose, and 5 µM catalase. To initiate catalysis 100 µL of NADPH-regenerating system was added. The final concentration of NADPH-regenerating system contained 3.25 mM glucose-6-phosphate, 41 µM $NADP^+$ and 0.55 U/mL glucose-6-phosphate-dehydrogenase. Reaction mixtures were incubated at 17 °C for 10 min (determined to be within the linear range of PebS activity). A spectrum was taken every 30 sec for 10 min. Crude bilins were extracted with a Sep-Pak Light C18 cartridge and subsequently evaporated to dryness using a SpeedVac concentrator. HPLC analysis was performed as described previously [4]. Concentration of protein and bilin was determined as described earlier [8].

Freeze-Quench electron paramagnetic resonance measurements — For electron paramagnetic resonance (EPR) measurements, the anaerobic assay described above was used with 4-fold

increased concentrations of PebS, BV, FNR and Fd, 15% spectro-analytical grade glycerol was included in the reaction mixtures. The total volume was 3 mL. At various times after addition of 200 µM NADPH, 200 µL aliquots were withdrawn from reaction mixtures, transferred to 4 mm quartz EPR tubes, and immediately frozen in liquid nitrogen. Continuous wave EPR studies of PebS were performed using a Bruker Elexsys E500 CW X-band EPR spectrometer. EPR spectra were acquired in a standard TE102 resonator at 40 K using a microwave frequency of 9.43 GHz, a power of 20 µW and a field modulation amplitude of 10 G. The temperature of the sample was maintained using an Oxford ESR900 liquid helium flow cryostat and an Oxford ITC 503 temperature controller.

Crystallization of PebS variants in complex with BV — Protein was concentrated to 7-12 mg/mL in 25 mM TES-KOH (pH 8.0), 100 mM KCl. Crystallization conditions were screened by the sitting drop vapor diffusion method using the Classic, Cryo, PEG and JSCG+ Suites (Qiagen), applying 200/100 nL and 100/100 nL mixtures of the protein solution/reservoir solution incubated at 18 °C in the dark. Initial hits were refined using the hanging drop technique. For the D105N variant final crystals diffracting to 2.2 Å were obtained using a reservoir containing 170 mM $(NH_4)_2SO_4$ and 20 % PEG 3350. Crystals were briefly soaked in motherliquor supplemented with 10 % PEG 400 before transfer into liquid N_2. Crystals for the D206N variant were grown using a reservoir containing 170 mM $(NH_4)_2SO_4$, 25 % PEG 8000, and 15 % glycerol. Crystals were directly transferred into liquid N_2 and diffracted to 1.85 Å.

Data collection and structure determination — Oscillation data of the D105N variant were collected at 100 K at the European Synchrotron Radiation Source (ESRF, Grenoble, France) on beamline ID23.2. Data of D206N variant crystals were collected at 100 K at the Swiss Light Source (SLS, Villigen, Switzerland) on beamline X10SA. All data were processed and scaled using the XDS package [14]. Data statistics are given in Table S1.
Both structures were solved by molecular replacement in Molrep using the structure of PebS with bound BV (Protein Data Bank code 2VGR) as search model.
The models were improved by iterating manual rebuilding in coot [15] and refinement using refmac [16] for the initial and phenix.refine [17] for the final cycles. Model and refinement statistics are given in Table S1. Non-crystallographic symmetry restraints were used throughout refinement and were only released for variable parts of the structures.

RESULTS

Anaerobic bilin reduction – In order to get a deeper insight into the PebS reaction mechanism, the anaerobic assay system described for other FDBRs was employed. In contrast to an aerobic assay this system allows the detection of possible bilin radical intermediates during the enzymatic reduction of BV and 15,16-DHBV by PebS and variants. The PebS reaction was started by the addition of reducing equivalents and resulted in a fast increase of absorbance at ~ 460 nm and ~ 740-760 nm. Concomitantly, a decrease of BV absorption at ~ 680 nm was observed (Fig. 2A, WT). Absorption at the indicated wavelengths is most likely due to the formation of bilin radical intermediates as shown for other FDBRs [5, 9, 10]. While the absorption of the putative radical intermediate(s) decreased during the course of the reaction, formation of the product PEB was observed at ~ 540 nm. Furthermore, the semi-reduced intermediate 15,16-DHBV becomes

temporarily visible at ~ 600 nm but disappears with the reaction proceeding (Fig. 2A). The final product of the PebS reaction is 3Z-PEB as confirmed by HPLC analysis (Fig. 2B).

Asp105 and Asp206 are critical protonating residues – Based on the PebS crystal structure the two conserved amino acid residues D105 and D206 were proposed to be crucial for PebS function, as their carboxy-groups are in hydrogen bonding distance to the substrate [13] and both residues are conserved in many members of the FDBR family. We therefore generated PebS variants in which the carboxy-group was changed to the corresponding amide (D105N and D206N), or in which the aspartate was replaced by the more extended glutamate (D105E and D206E). In our anaerobic assay incubation of D105N with BV and an excess of electron equivalents resulted in an absorption increase at ~ 460 nm and ~ 740-760 nm similar to WT, but with a very slow decay. These results suggest the formation of bilin radical intermediates and their stabilization/ accumulation by the variant (Fig. 2A). Subsequent HPLC analyses revealed that this variant is unable to convert the substrate BV (Fig. 2B). Interestingly, the D105E variant fully retained the ability to catalyze the first reduction at the 15,16-methine bridge, but could not catalyze the second reduction at the A-ring 2,3,3^1,3^2-diene system, thereby yielding 15,16-DHBV as the final product (Fig. 2).

Investigation of PebS_D206N with BV as the substrate showed a decrease of BV absorption at ~ 680 nm with subsequent increase and decrease of a possible bilin radical absorption at ~ 460 nm and ~ 740-760 nm. HPLC analyses of this variant demonstrated that only the first reduction step was performed. The final product of this reaction with a maximum absorption at ~ 605 nm is 15,16-DHBV (Fig. 2). The same product was obtained when D206 was exchanged by a glutamic acid residue (data not shown). However, in this variant the reaction can be pushed further to produce PEB by a ten-fold increased concentration of FNR (Fig. 2).

Catalytic turnover was also tested with the intermediate of the reaction, 15,16-DHBV. As expected, none of the asparagine variants was able to convert 15,16-DHBV whereas the WT protein catalyzed the formation of PEB (indicated by an absorption increase at ~ 540 nm; data not shown). Interestingly, UV-Vis spectra of the catalytic turnover of these variants with 15,16-DHBV as the substrate showed no indication of absorbance that could point to the formation of a 15,16-DHBV radical intermediate (data not shown). In this regards it has to be noted that externally applied 15,16-DHBV to D206N revealed a 60 nm spectral shift to the shorter wavelength of the UV-Vis spectrum as compared to the enzymatically produced and enzyme bound 15,16-DHBV (Fig. S1).

Bilin radical intermediates during PebS reaction – Since the performed anaerobic assays suggested the formation of bilin radical intermediates and their accumulation in the D105N variant, additional anaerobic bilin reductase assays were performed using an excess of NADPH as the reducing agent and 40 µM of the PebS-BV complex. The reactions were monitored via UV-Vis (Fig. S2) and EPR spectroscopy (Fig. 3). For this aliquots were taken at different time points and flash frozen for further EPR measurements. Paramagnetic species could be detected for PebS_WT and the variants D105N and D206N, indicated by an isotropic EPR signal at g~2 with a first derivative peak to peak linewidth of about 15 G (Fig. 3). The PebS_WT protein incubated with BV showed a fast increase and decay of the detectable radical with the strongest signal being observed after 0.5 min. The PebS_D105N variant generated a relatively stable paramagnetic intermediate as shown by an increasing EPR signal with no significant decrease (Fig. 3, middle panel). The PebS_D206N variant showed a similar behavior of radical signal increase and decrease in the course of the reaction as observed for the WT reaction. At the end of the reaction at 20 min a weak signal was still detectable either due to weak radical stabilization or an uncompleted reaction (Fig. 3, right panel).

Absorption changes at the long and short wavelength (~ 460 nm, ~ 740-760 nm) which do not correspond to the substrate (BV) or product (DHBV, PEB) absorption maxima followed similar kinetics as the EPR signal (Fig. 4). For comparison, the time point with the highest EPR intensity has been assigned as 100 %. Since the EPR linewidth of the radical signal was invariant over the course of the experiment, the EPR signal intensities were taken as the peak to peak amplitudes of the first derivative signals as presented in Fig. 3. Relative EPR signal intensity and absorbance at 760 nm were normalized to the amplitude of the signal at 0.5 min for PebS_WT reaction and at 2.5 min for the reaction of the two variants, respectively. As shown in Fig. 4 the EPR intensity followed very similar kinetics as the absorbance change at 760 nm. Therefore, absorption at this wavelength can most likely be attributed to the formation of bilin radical intermediates. These results confirm a radical mechanism of BV reduction catalyzed by PebS. Unfortunately, similar experiments employing 15,16-DHBV as a substrate to detect paramagnetic species of the second reduction catalyzed by PebS were technically not feasable due to the high amount of 15,16-DHBV required for the analysis.

Structure of the PebS variants D105N and D206N – In addition to the biochemical evidence that both aspartate residues are critical for catalysis, the respective asparagine variants were crystallized to obtain structural information to help elucidate the underlying catalytic mechanism. X-ray data of PebS_D105N and PebS_D206N with bound BV have been collected. The structure of PebS_D105N (PDB code 2X9I) was refined at 2.2 Å resolution and PebS_D206N (PDB code 2X9J) at 1.85 Å. Both variants show the identical overall fold as observed for PebS_WT (RMSD around 0.27 Å for approx 190 Cα-atoms for all observed domains) (Fig. S3).

In all PebS structures the substrate BV is bound in a pocket parallel to the central β-sheet with the propionate side chains facing the solvent. As already observed for the WT structures, the amino acid residues located on the proximal β-sheet side define the rigid part of the active site. In contrast residues on the distal side are more flexible (Fig. 5 and Fig. S4). Accordingly, residue D105 and the respective N105 variant superimpose perfectly (Fig. 5A and Fig. S4A, B). D206, on the other hand has been found in three different conformational modes in our PebS_WT structures. In one conformation D206 faces the solvent ("out"). In the second, dominant conformation D206 coordinates the substrate indirectly via a central pyrrole water ("in"). In the third conformation observed in the WT enzyme D206 directly coordinates the pyrrole nitrogens and effectively displaces the pyrrole water ("deep"). Using this nomenclature, both copies of the D206N variant in the asymmetric unit are in the "in" conformation. In the D105N structure we find four copies in the asymmetric unit, two of which have D206 in the "deep" conformation and two in the "in" conformation (Table S2). In one of the latter we did not find electron density to support the placement of the pyrrole water. In both PebS variants BV is found exclusively in the porphyrin-like planar form.

DISCUSSION

PebS is a phage-derived FDBR involved in the biosynthesis of PEB, one of the main chromophores in cyanobacterial light-harvesting complexes. So far PebS activity is solely found in the enzyme derived from the marine cyanophage P-SSM2 infecting low-light-adapted *Prochlorococcus* strains [11]. Putative PebS orthologs have been identified in sequenced cyanophage genomes and in metagenome-derived sequences of phage origin only [12, 18]. In a first two-electron reduction step PebS regiospecifically reduces the 15,16 methine bridge of BV forming the intermediate 15,16-DHBV. 15,16-DHBV is further reduced to PEB at the A-ring 2,3,3^1,3^2-diene structure in a second two-electron reduction step. Both reduction steps generate

two new chiral C-atoms at position C-2 and C-16, both of which are in the *R* configuration [19]. This second reduction step also formally resembles the second reduction catalyzed by PcyA and the reaction catalyzed by HY2 as they all target the same structure at the tetrapyrrole's A-ring but use different substrates (15,16-DHBV (PebS), 18^1,18^2-DHBV (PcyA) and BV (HY2)).

The sole product of the PebS reaction is 3Z-PEB – Improvement of our assay work-up conditions enabled us to ultimately prove that the sole product of the PebS reaction is the *3Z*-isomer of PEB. Although we previously had indications from UV-Vis spectroscopy that this is the case [13], HPLC analyses now clearly show that *3Z*-PEB is the final product (Fig. 2B). Therefore, the occurrence of the *3E*-isomer is simply due to experimental artefacts like assay-workup conditions at slightly higher temperatures [3]. Unpublished data from our laboratory furthermore suggest similar results for PcyA, were the *3Z*-isomer of PCB is the sole product (Busch & Frankenberg-Dinkel, unpublished results). Earlier results from phytochromobilin synthase from oats and other FDBRs from *Cyanidium caldariorum* also confirmed the production of the *3Z*-isomer [20-22]. Therefore, we propose that all FDBRs only produce the *3Z*-isomer.

PebS acts via a radical mechanism – Since one common feature of all FDBRs is the lack of any metal or organic cofactors the presence of bilin radical intermediates was proposed [3]. Radical species could already be confirmed for PcyA [5] and HY2 [9]. Here we show that PebS also acts via bilin radical intermediates which makes them a specific feature of this family of enzymes [5, 9]. Employing the anaerobic assay system in combination with UV-vis spectroscopy these radical species can be observed by their distinct absorption bands in the long and short wavelength range. During the course of the PebS reaction the observed signal emerges from different radical species that cannot be distinguished here since the reaction likely proceeds via a concerted proton-coupled electron transfer.

Asp105 and Asp206 are both proton donating residues in the PebS reaction – A strong accumulation of radical intermediate was observed for the variant D105N. Since this variant is unable to catalyze the conversion of BV, it is catalytically stalled in one of the protonations of the first reduction. The observed radical is therefore most likely one of the two radicals occurring in the first two-electron reduction of BV to 15,16-DHBV. This finding is in agreement with studies on PcyA where the homologous amino acid exchange leads to a loss of activity and also to BV radical stabilization [23]. In contrast, D206N is still able to convert BV to the intermediate 15,16-DHBV and therefore is only essential for A-ring reduction. This is consistent with observations for plant PΦB synthase (HY2) which catalyzes the two-electron reduction of the BV A-ring to PΦB. Here the D206 homologue D256 has been found to be essential for BV reduction as well [9]. While PcyA also contains an aspartate residue at this position, its mutation to Asn has only a minimal effect on activity [23]. Therefore it is not surprising that this residue is found in the "out" position in the PcyA crystal structure [24]. This conserved residue seems to play a special role in both A-ring reductions of HY2 and PebS but not in PcyA. In this regard, PcyA is the only member of the FDBR family where this amino acid residue is not strictly conserved (see Fig. S5). Alternative residues are found in PcyA of *Prochlorococcus marinus* MED4 (Glu) and the cyanophage P-SSM4 (Lys). Both enzymes were shown to be catalytically active and produce PCB [12, 25]. Another fundamental difference between the PcyA and PebS structures is the existence of a continuous proton uptake channel (proton relay) leading to a conserved His88 residue in PcyA. This channel plays a central role in the PcyA reaction scheme and has been proposed to be important for reprotonation of D105 [10]. Therefore, although we find certain structural features to be conserved within the whole FDBR family no common catalytic mechanism can be proposed.

Proposed catalytic mechanism of PebS – Based on our biochemical, biophysical and structural data we propose the following catalytic mechanism for PebS (Fig. 6A). The bound bilins will always be present as a mixture of tautomers (lactim-lactam) regarding the location of the protons. We envisage the first event of the reaction being a protonation of a mono-lactim BV (in the ACδ configuration[1]) through the pyrrole water (H_2O). The resulting monohydrobiliverdin cation will take up an electron from Fd and generate a neutral monohydrobiliverdin radical (ACDδ). Residue D105 will be important for the next concerted proton-electron transfer and also for directing the proton stereospecifically to C-16 to generate the *R* configuration at this carbon atom. We envisage that the latter might be possible through a D105 mediated stereospecific tautomerization (indicated by a black asterisk in Fig. 6A) to yield 15,16-DHBV. We expect that PebA will work in a similar fashion with D105 being the critical proton donating residue. This scheme would also suggest that a D105N mutant accumulates a neutral monohydrobiliverdin radical. The nature of this radical will be further investigated by future high field EPR measurements.

D206 has been found to be flexible (ranging from an "out" to a "deep" in conformation in direct contact with the BV) and to be essential for the second reduction step of PebS. Including this information in our mechanism we propose an initial protonation of a 15,16-DHBV monolactim (αCD) from D206 to generate a trihydrobiliverdin cation, concurrent electron transfer from Fd will result in a neutral radical (αBCD). Next would be the stereospecific protonation of C-2. Again, D105 could play a crucial role in this step. The still deprotonated D105 could catalyze a stereospecific tautomerization yielding a neutral lactam radical (BCD). The final step could be a concerted proton-electron transfer followed by a final tautomerization. The exact nature of which is still unknown but could possibly again involve D206 and water molecules. We would envisage that the homologous aspartic acid residues D107 and D231 of PebB from *Synechococcus* sp. WH8020 are also crucial for the PebB reaction. However, the initial protonation state of D107 in PebB is currently unknown and is subject of current investigation in our laboratory.

One has to note that due to the reduced extent of the conjugated π-system the reaction intermediate 15,16-DHBV will adopt a different conformation in the active site than the BV found in our "ground state" structures. In addition, the D105E variant, which retains the catalytically critical carboxy group, can still catalyze the first, but not the second reduction. The longer side chain changes the geometry of the active site thereby hindering the productive positioning of the reaction intermediate 15,16-DHBV.

Clearly more work is needed to clarify the structural changes involved in these intermediates, both by analyzing the two glutamate variants, and the accumulated radicals of PebS.

In summary, the following points would be fundamental for the proposed mechanism: I) Electron transfer from Fd is directly coupled to proton transfer from water or the protein. II) Tautomerization of the different protonation states of the substrate occurs constantly. III) Stereospecific reduction in both steps is enforced by D105. IV) Flexibility of D206 facilitates water release and re-protonation.

[1] for nomenclature the authors refer to Ref. [26]

REFERENCES

1 Glazer, A. N. (1985) Light Harvesting by Phycobilisomes. Ann Rev Biophys Biophys Chem. **14**, 47-77

2 Cornejo, J., Willows, R. D. and Beale, S. I. (1998) Phytobilin biosynthesis: cloning and expression of a gene encoding soluble ferredoxin-dependent heme oxygenase from *Synechocystis* sp. PCC 6803. Plant J. **15**, 99-107

3 Frankenberg, N., Mukougawa, K., Kohchi, T. and Lagarias, J. C. (2001) Functional genomic analysis of the HY2 family of ferredoxin-dependent bilin reductases from oxygenic photosynthetic organisms. Plant Cell. **13**, 965-978

4 Frankenberg, N. and Lagarias, J. C. (2003) Phycocyanobilin:ferredoxin oxidoreductase of *Anabaena* sp. PCC 7120. Biochemical and spectroscopic. J Biol Chem. **278**, 9219-9226

5 Tu, S. L., Gunn, A., Toney, M. D., Britt, R. D. and Lagarias, J. C. (2004) Biliverdin reduction by cyanobacterial phycocyanobilin:ferredoxin oxidoreductase (PcyA) proceeds via linear tetrapyrrole radical intermediates. J Am Chem Soc. **126**, 8682-8693

6 Dammeyer, T. and Frankenberg-Dinkel, N. (2008) Function and distribution of bilin biosynthesis enzymes in photosynthetic organisms. Photochem Photobiol Sci. **7**, 1121-1130

7 Kohchi, T., Mukougawa, K., Frankenberg, N., Masuda, M., Yokota, A. and Lagarias, J. C. (2001) The Arabidopsis HY2 gene encodes phytochromobilin synthase, a ferredoxin-dependent biliverdin reductase. Plant Cell. **13**, 425-436

8 Dammeyer, T. and Frankenberg-Dinkel, N. (2006) Insights into phycoerythrobilin biosynthesis point toward metabolic channeling. J Biol Chem. **281**, 27081-27089

9 Tu, S. L., Chen, H. C. and Ku, L. W. (2008) Mechanistic Studies of the Phytochromobilin Synthase HY2 from Arabidopsis. J Biol Chem. **283**, 27555-27564

10 Tu, S. L., Rockwell, N. C., Lagarias, J. C. and Fisher, A. J. (2007) Insight into the radical mechanism of phycocyanobilin-ferredoxin oxidoreductase (PcyA) revealed by X-ray crystallography and biochemical measurements. Biochemistry. **46**, 1484-1494

11 Sullivan, M. B., Coleman, M. L., Weigele, P., Rohwer, F. and Chisholm, S. W. (2005) Three Prochlorococcus cyanophage genomes: signature features and ecological interpretations. PLoS Biol. **3**, e144

12 Dammeyer, T., Bagby, S. C., Sullivan, M. B., Chisholm, S. W. and Frankenberg-Dinkel, N. (2008) Efficient phage-mediated pigment biosynthesis in oceanic cyanobacteria. Curr Biol. **18**, 442-448

13 Dammeyer, T., Hofmann, E. and Frankenberg-Dinkel, N. (2008) Phycoerythrobilin Synthase (PebS) of a Marine Virus: crystal structures of the biliverdin complex and the substrate -free form J Biol Chem. **283**, 27547-27554

14 Kabsch, W. (1993) Automatic processing of rotation diffraction data from crystals of initially unknown symmetry and cell constants. J Appl Cryst. **26**, 795-800

15 Emsley, P. and Cowtan, K. (2004) Coot: model-building tools for molecular graphics. Acta Crystal Sec D. **60**, 2126-2132

16 Murshudov, G. N., Vagin, A. A. and Dodson, E. J. (1997) Refinement of macromolecular structures by the maximum-likelihood method. Acta Crystal Sec D. **53**, 240-255

17 Adams, P. D., Grosse-Kunstleve, R. W., Hung, L.-W., Ioerger, T. R., McCoy, A. J., Moriarty, N. W., Read, R. J., Sacchettini, J. C., Sauter, N. K. and Terwilliger, T. C. (2002) PHENIX: building new software for automated crystallographic structure determination. Acta Crystal Sec D. **58**, 1948-1954

18 Sullivan, M. B., Huang, K. H., Ignacio-Espinoza, J. C., Berlin, A. M., Kelly, L., Weigele, P. R., Defrancesco, A. S., Kern, S. E., Thompson, L. R., Young, S., Yandava, C., Fu, R.,

Krastins, B., Chase, M., Sarracino, D., Osburne, M. S., Henn, M. R. and Chisholm, S. W. (2010) Genomic analysis of oceanic cyanobacterial myoviruses compared with T4-like myoviruses from diverse hosts and environments. Environ Microbiol. **in press**

19 Gossauer, A. and Weller, J. P. (1978) Synthesis of bile pigments. 9. Chemical total synthesis of (+)-(2R,16R)- and (+)-(2S,16R)-phycoerythrobilin dimethyl ester. J Am Chem Soc. **100**, 5928-5933

20 Beale, S. I. and Cornejo, J. (1984) Enzymic transformation of biliverdin to phycocyanobilin by extracts of the unicellular red alga *Cyanidium caldarium*. Plant Physiol. **76**, 7-15.

21 Beale, S. I. and Cornejo, J. (1991b) Biosynthesis of phycobilins. 3(Z)-Phycoerythrobilin and 3(Z)-phycocyanobilin are intermediates in the formation of 3(E)-phycocyanobilin from biliverdin IXa. J Biol Chem. **266**, 22333-22340

22 McDowell, M. T. and Lagarias, J. C. (2001) Purification and biochemical properties of phytochromobilin synthase from etiolated oat seedlings. Plant Physiol. **126**, 1546-1554

23 Tu, S. L., Sughrue, W., Britt, R. D. and Lagarias, J. C. (2006) A conserved histidine-aspartate pair is required for exovinyl reduction of biliverdin by a cyanobacterial phycocyanobilin:ferredoxin oxidoreductase. J Biol Chem. **281**, 3127-3136

24 Hagiwara, Y., Sugishima, M., Takahashi, Y. and Fukuyama, K. (2006) Crystal structure of phycocyanobilin:ferredoxin oxidoreductase in complex with biliverdin IXa, a key enzyme in the biosynthesis of phycocyanobilin. Proc Natl Acad Sci U S A. **103**, 27-32

25 Dammeyer, T., Michaelsen, K. and Frankenberg-Dinkel, N. (2007) Biosynthesis of open-chain tetrapyrroles in *Prochlorococcus marinus*. FEMS Microbiol Lett. **271**, 251-257

26 Stoll, S., Gunn, A., Brynda, M., Sughrue, W., Kohler, A. C., Ozarowski, A., Fisher, A. J., Lagarias, J. C. and Britt, R. D. (2009) Structure of the biliverdin radical intermediate in phycocyanobilin:ferredoxin oxidoreductase identified by high-field EPR and DFT. J Am Chem Soc. **131**, 1986-1995

ACKNOWLEDGEMENT

We also would like to thank the beamline staff at the European Synchrotron Radiation Facility (ESRF, Grenoble) and the Swiss Light Source (SLS, Villigen) and colleagues from the Max-Planck Institute for Physiology (Dortmund) for help during data collection. Thanks are due to Dr. Shih-Long Tu for his help in setting up the anaerobic assay system in our laboratory and to Dr. Jessica Wiethaus for helpful discussion.

FUNDING

This work was financially supported by the SFB 480 (Teilprojekt C6 and C8) from the Deutsche Forschungsgemeinschaft to NFD and EH. AB received a PhD fellowship of the Ruhr-University Bochum Research School.

SUPPORTING INFORMATION

Two supplementary Tables and five supplementary Figures are available online.

FIGURE LEGENDS

Figure 1. Bilin biosynthesis pathway
The substrate BV is reduced in two- and four-electron reduction steps by the FDBRs. Synthesis of the plant chromophore PΦB requires a two-electron reduction by HY2. In cyanobacteria PebA reduces BV to 15,16-DHBV which is further reduced to PEB catalyzed by PebB. Phage derived PebS catalyzes the four-electron reduction from BV to PEB with 15,16-DHBV as the intermediate. PcyA also performs a formal four-electron reduction to PCB with 18^1, 18^2-DHBV as the intermediate.

Figure 2. Absorption spectra under anaerobic conditions (A) and HPLC analyses (B) of WT_PebS and variants
10 µM of PebS-BV complex was used and absorption spectra were monitored for 10 min every 30 sec. The reaction was started by addition of an NADPH regenerating system. The reaction was stopped and the products analyzed via HPLC at 380 nm (solid line) and 560 nm (dashed line). **A.** Time course of substrate conversion. BV absorption due to reduction decreases at 680 nm, 15,16-DHBV formation results in an absorption increase at 605 nm, PEB increases with an absorption at 540 nm. Absorption of ~460 nm, ~740 nm and ~760 nm increases with further decrease for PebS_WT and PebS_D206N/E and PebS_D105E indicated through double arrows and is stable in the case of PebS_D105N. **B.** HPLC analyses were conducted with C18 reverse phase columns from Phenomenex. The Ultracarb 5µ column was used for all variants and the WT, except for PebS_D105E and PebS_D206E where the Luna 5µ column was used. Retention times for the two columns slightly differ. The reaction products DHBV and PEB were detected at 560 nm. BV was detected at 380 nm. Products were confirmed by retention times of bilin standards and whole spectrum analysis of elution peaks. Asterisks indicate unspecific degradation products.

Figure 3. EPR measurement of bilin radicals occurring during reactions of PebS with BV
EPR spectroscopic measurement of BV complexes of PebS_WT, PebS_D105N and D206N_PebS variant. Samples were withdrawn before addition of NADPH and 0.5 min, 2.5 min, 4.5 min and 20 min after the reaction was started and were immediately frozen in liquid nitrogen. All spectra are on the same scale and were recorded at 40 K, 20 µW power and 10 Gauss field modulation (see text for further experimental details).

Figure 4. Correlation of EPR signal and absorption at 760 nm
EPR signal intensity (black bar) was calculated from the first derivative peak to peak amplitude and compared to the absorption change at 760 nm (white bar) during the reaction with BV. The time point of strongest EPR signal was set to 100 %. Relative absorbance at 760 nm and EPR signal intensity were normalized to the time point at 0.5 min (PebS_WT) and 2.5 min (PebS_D105N, PebS_D206N).

Figure 5. Superposition of the active site of the WT, the D105N (A) and D206N (B) variant with bound substrate BV

The WT is shown in grey and the variants in red (D105N) and blue (D206N). Only the residues at position 105, 206 and 88 are shown. The hydrogen bonding network is only shown for the variants.

Figure 6. PebS-catalyzed reduction of BV IXα. A. Proposed mechanism. Black stars indicate stereospecific reductions. See text for details. **B.** Illustration for the used nomenclature of protonation sites in the substrate BV. The pyrrole nitrogens are denoted A, B, C, and D, whereas the two carbonyl-oxygenas on the A- and D-ring are denoted α and δ. Nomenclature was adaped from [26].

Biochemical Journal Immediate Publication. Published on 04 Nov 2010 as manuscript BJ20101642

Figure 1 Busch et al

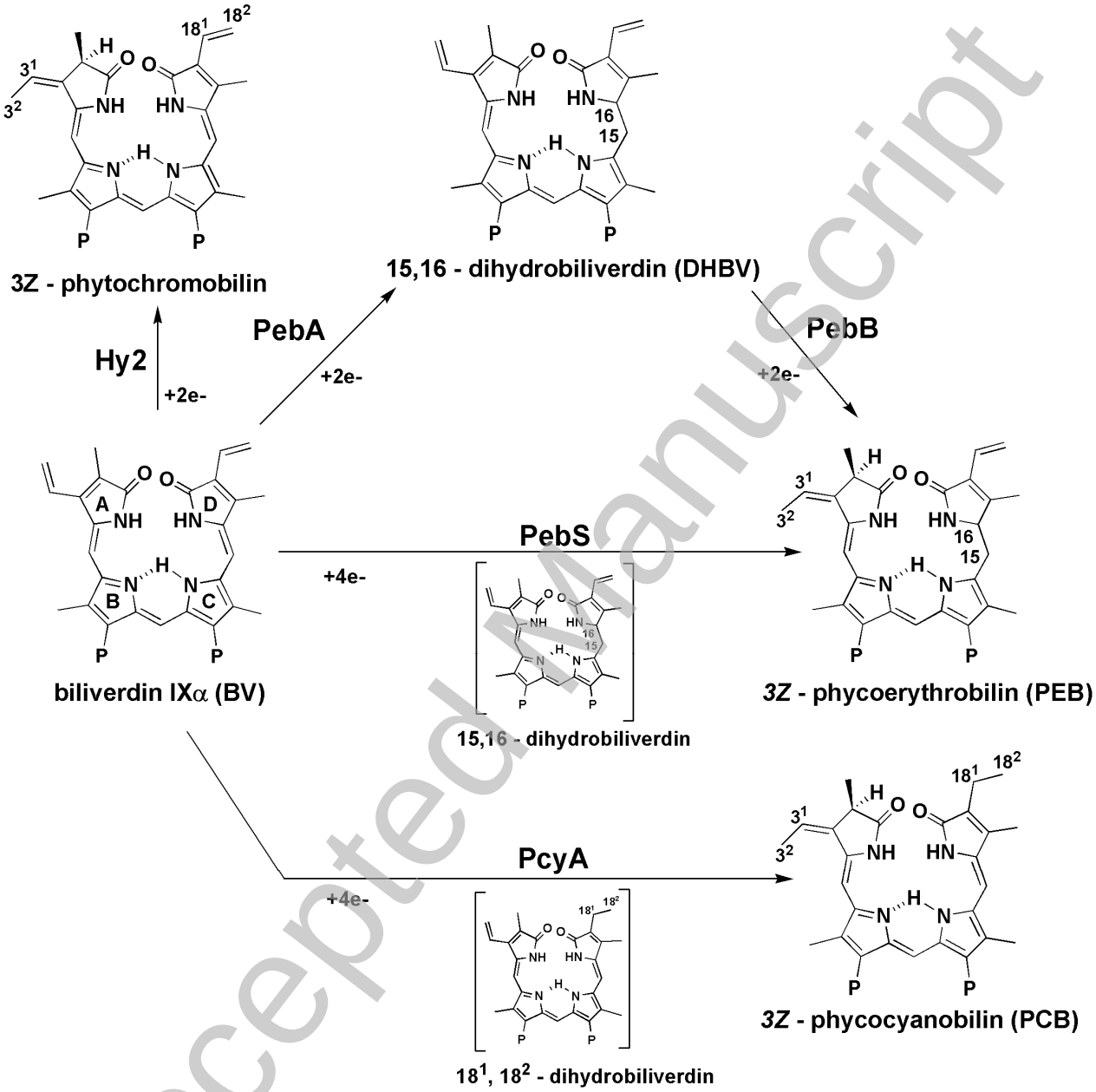

Figure 2. Busch et al.

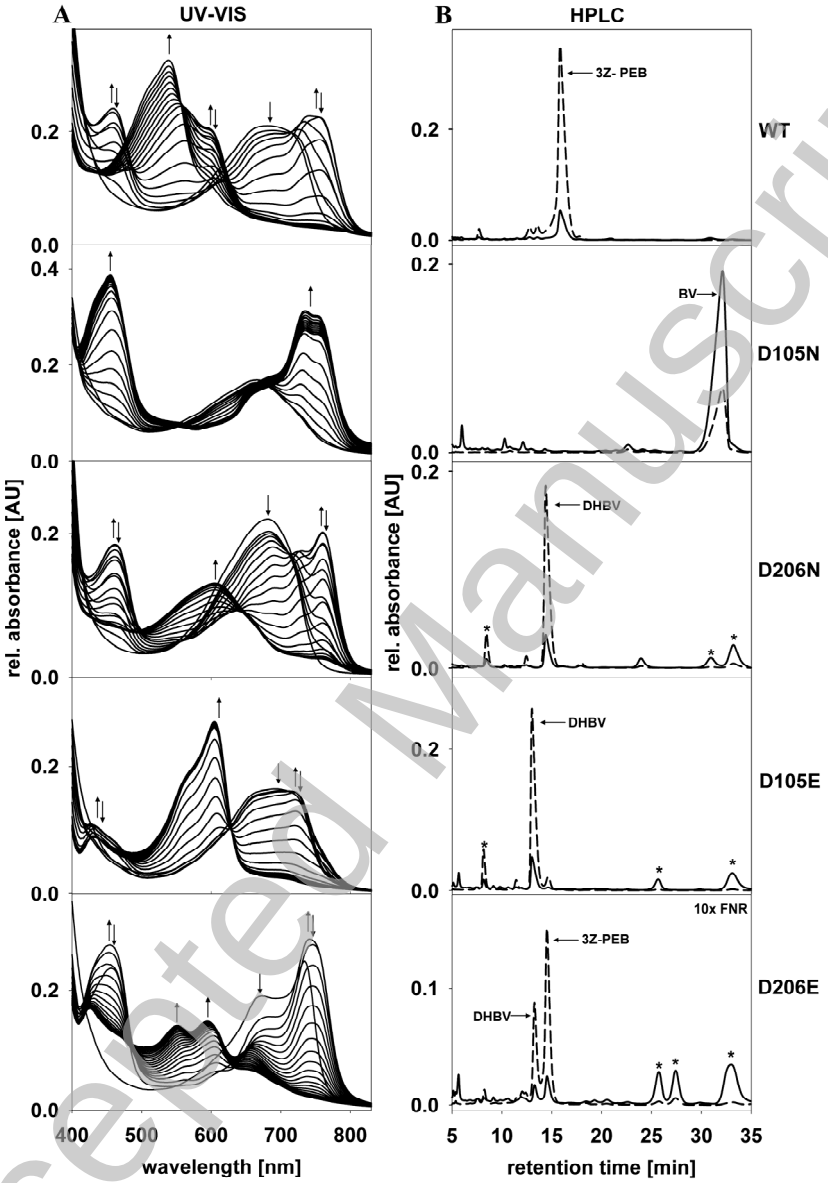

Figure 3. Busch et al.

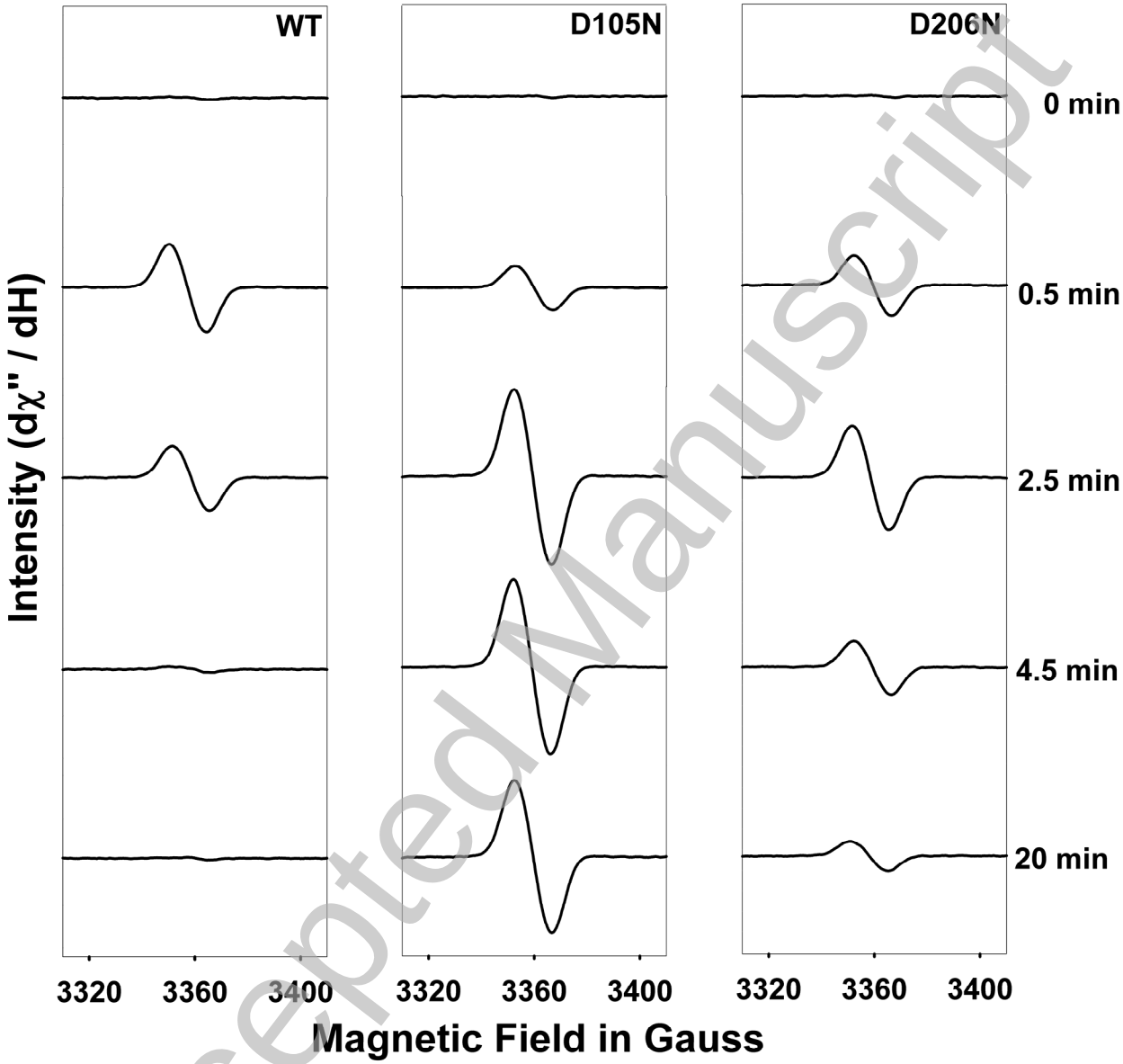

Figure 4. Busch et al.

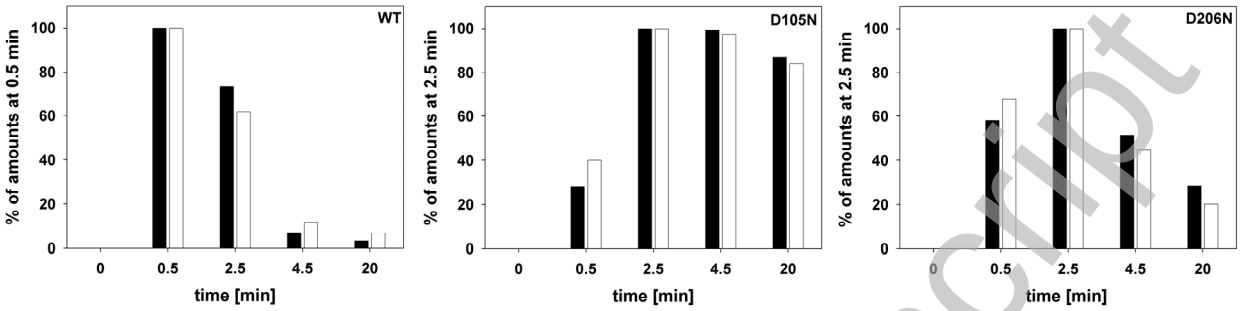

Figure 5. Busch et al.

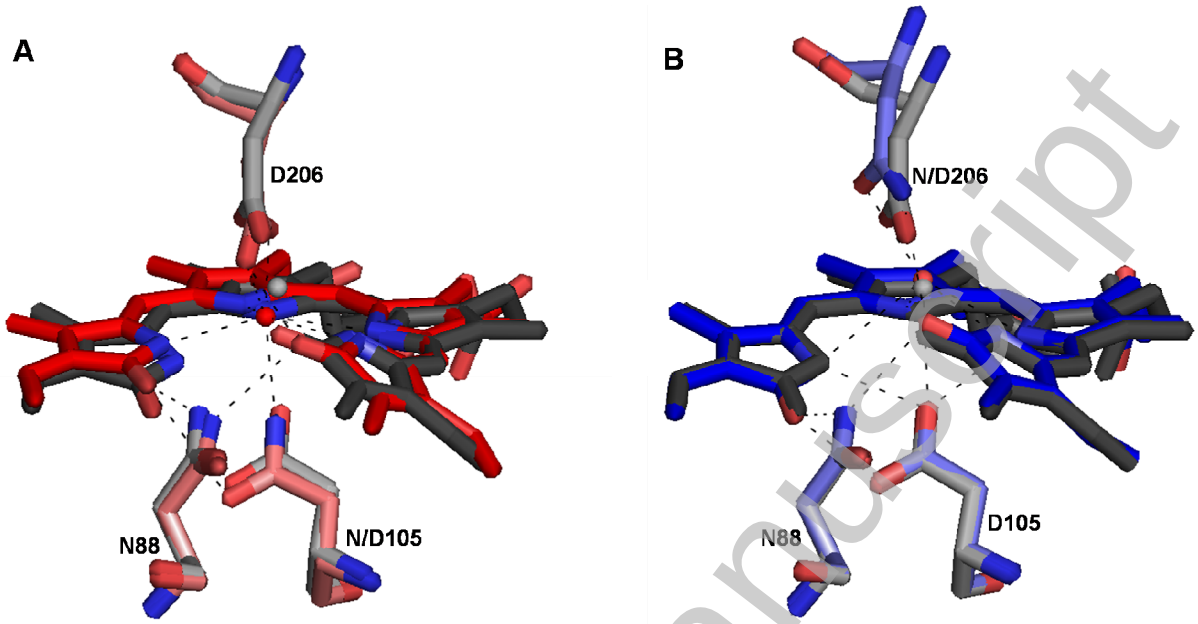

Biochemical Journal Immediate Publication. Published on 04 Nov 2010 as manuscript BJ20101642

Figure 6. Busch et. al.